Available online at www.sciencedirect.com
SCIENCE DIRECT®
Marine Geology 201 (2003) 269–286
MARINE GEOLOGY
INTERNATIONAL JOURNAL OF MARINE GEOLOGY, GEOCHEMISTRY AND GEOPHYSICS
www.elsevier.com/locate/margeo

Characteristics of gas hydrate occurrences associated with mud diapirism and gas escape structures in the northwestern Sea of Okhotsk

T. Lüdmann *, H.K. Wong

Institute of Biogeochemistry and Marine Chemistry, University of Hamburg, Bundesstrasse 55, 20146 Hamburg, Germany

Received 21 June 2002; accepted 17 July 2003

Abstract

An interpretation of 8450 line-km of seismic reflection data acquired during four cruises in the northwestern Sea of Okhotsk shows widespread occurrence of free gas or gas hydrates in the sediment. This occurrence is documented seismically by gas escape structures, acoustic blanking, and by a bottom simulating reflector (BSR). Gas escape structures and vents are concentrated on the northern Sakhalin continental margin. Here, they are associated with local tectonic movements along a N–S trending dextral shear system (the Inessa Shear Zone). Mud diapirism is common in the Derugin Basin where compression dominates. This diapirism is probably closely related to the gas accumulations in the sediment below the base of the gas hydrate stability zone (BGHSZ). Conductive heat flow derived from the BSR depth distribution averages about 30 ± 8 mW m^{-2}. Only adjacent to basement highs and around the Inessa Shear Zone do values higher than 80 ± 22 mW m^{-2} occur. These high values are attributed to an elevated geothermal gradient in the tectonically active zone where fluid venting takes place. Areas of drift sedimentation and mass wasting, where sedimentation rates are high, are characterised by computed heat flow values below 30 ± 8 mW m^{-2}. However, these values must be corrected upwards by 3–20% depending on the sedimentation rate applicable (3.8–100 cm/kyr). The total amount of methane preserved in the hydrate stability zone (HSZ) and trapped as free gas beneath the BSR is estimated at $17 \pm 14 \times 10^{12}$ m^3 for the northwestern Sea of Okhotsk and $15 \pm 12 \times 10^{13}$ m^3 for the entire Sea of Okhotsk. The latter figure represents about 0.8% of the global reservoir of methane gas from hydrates. Our study documents that the semi-enclosed Sea of Okhotsk offers favourable conditions for the accumulation of gas in its sediments on account of its subarctic climate and the prevailing hydrologic regime. These conditions include high primary productivity, low bottom water temperatures and high sedimentation rates.

Keywords: gas hydrate; methane; heat flow; mud diapirism; BSR; Sea of Okhotsk

1. Introduction

KOMEX (Kurile-Sea of Okhotsk Marine Experiment) is a joint German–Russian research project aimed at a multi-disciplinary study of the geological evolution, palaeoceanography, and

* Corresponding author. Tel.: +49-40-42838-6335; Fax: +49-40-42838-6347.
E-mail address: luedmann@geowiss.uni-hamburg.de (T. Lüdmann).

0025-3227/03/$ – see front matter © 2003 Elsevier B.V. All rights reserved.
doi:10.1016/S0025-3227(03)00224-X

vent phenomena of the Sea of Okhotsk. One of the KOMEX geophysical study areas lies in the northwestern Sea of Okhotsk with the Derugin Basin at its centre (Fig. 1). It is bounded to the west by the northern Sakhalin continental slope, and to the north by the Staretsky Trough and the Kashevarov Bank of the North Okhotsk margin.

In the winter, under the influence of a subarctic climate, 75% of the Sea of Okhotsk is covered by an ice sheet averaging 1 m in thickness. Ice formation and the accompanying brine release produces cold saline waters of the basin-wide, 100-m-thick, subzero (−1.5°C) dichothermal layer that lies between 50 and 150 m below the sea surface (Kitani, 1973; Talley and Nagata, 1995). The average temperature of the water column is about 2°C. The sediments in the Derugin Basin are dominated by ice-rafted detritus, mass wasting deposits and hemipelagics of high organic content because of the high primary productivity (Sancetta, 1981; Gorbarenko et al., 1990; Gorbarenko, 1991; Botsul et al., 1999; Astakhov et al., 2000; Shiga and Koizumi, 2000; Wong et al., in press). Major source of sediments is the Amur River (inset, Fig. 1); its sedimentary load is redistributed at the Sakhalin continental margin by strong southward flowing bottom currents and gravitational downslope processes (Wong et al., in press).

Gas accumulation in the sediments of the semi-enclosed Sea of Okhotsk is made favourable by the subarctic climate and the prevailing hydrologic regime, which result in high primary productivity, low bottom water temperatures and high sedimentation rates (3.8–100 cm/kyr; Gorbarenko et al., 1990; Botsul et al., 1999; Astakhov et al., 2000). Regions where gas hydrates are associated with gas seepage fields include areas offshore of Paramushir Island (inset, Fig. 1) and on the northeastern Sakhalin continental slope (Fig. 1) (Cranston et al., 1994; Soloviev and Ginsburg, 1994; Basov et al., 1996; Gaedicke et al., 1997; Soloviev and Ginsburg, 1997). Gas hydrates have been sampled in both of these areas in gravity cores.

Because gas dispersed in the subsurface leads to attenuation of the seismic energy, gas-saturated deposits are often characterised by zones of acoustic masking and wipeout of the primary stratifications (Yun et al., 1999). The so-called bottom simulating reflector (BSR) marks the base of the thermobaric gas hydrate stability zone (BGHSZ). It is generated by the large impedance contrast between high-velocity gas hydrate-cemented sediments and low-velocity free gas beneath (Stoll and Bryan, 1979; Hyndman and Spence, 1992). However, results from ODP Leg 164 indicate that gas hydrates are present in the hydrate stability zone (HSZ) even where a BSR is absent and that the impedance contrast generating the BSR is principally caused by gas, not hydrate (Holbrook et al., 1996). According to the seismic study of Hyndman and Spence (1992), a BSR can appear without free gas below the BGHSZ if gas hydrate fills more than 30% of the pore space.

A BSR is observed on almost all seismic lines in the research area below a water depth of c. 250 m. In this study, we focussed our attention on the geophysical signatures of gas accumulations in the sediments and the associated gas escape structures in the northwestern Sea of Okhotsk. Additionally, we made a first attempt to quantify the amount of methane gas associated with these extensive gas and gas hydrate occurrences.

Another widespread phenomenon in the Sea of Okhotsk is mud diapirism. Our studies suggest that it is closely related to the production of free gas below the BHGSZ. It may also have resulted from the prevailing high sedimentation rates which lead to over-pressuring of the sediments during disequilibrium compaction.

2. Acquisition and processing of seismic data

Within the framework of the German–Russian joint KOMEX project, four reflection seismic surveys have been carried out in the northwestern Sea of Okhotsk (Fig. 1). A total of 8450 km of seismic reflection data were obtained. These cruises are: cruise 16 of the R/V *Professor Lavrentyev* (GERDA: *Geophysical Research in the Derugin Basin Area*, in 1995), cruise 22 of R/V *Professor Gagarinsky* (INESSA: *Investigations of Eastern Sakhalin Shelf Areas*, in 1998), cruise 26 of R/V *Professor Gagarinsky* (SAKURA: *Kurile–*

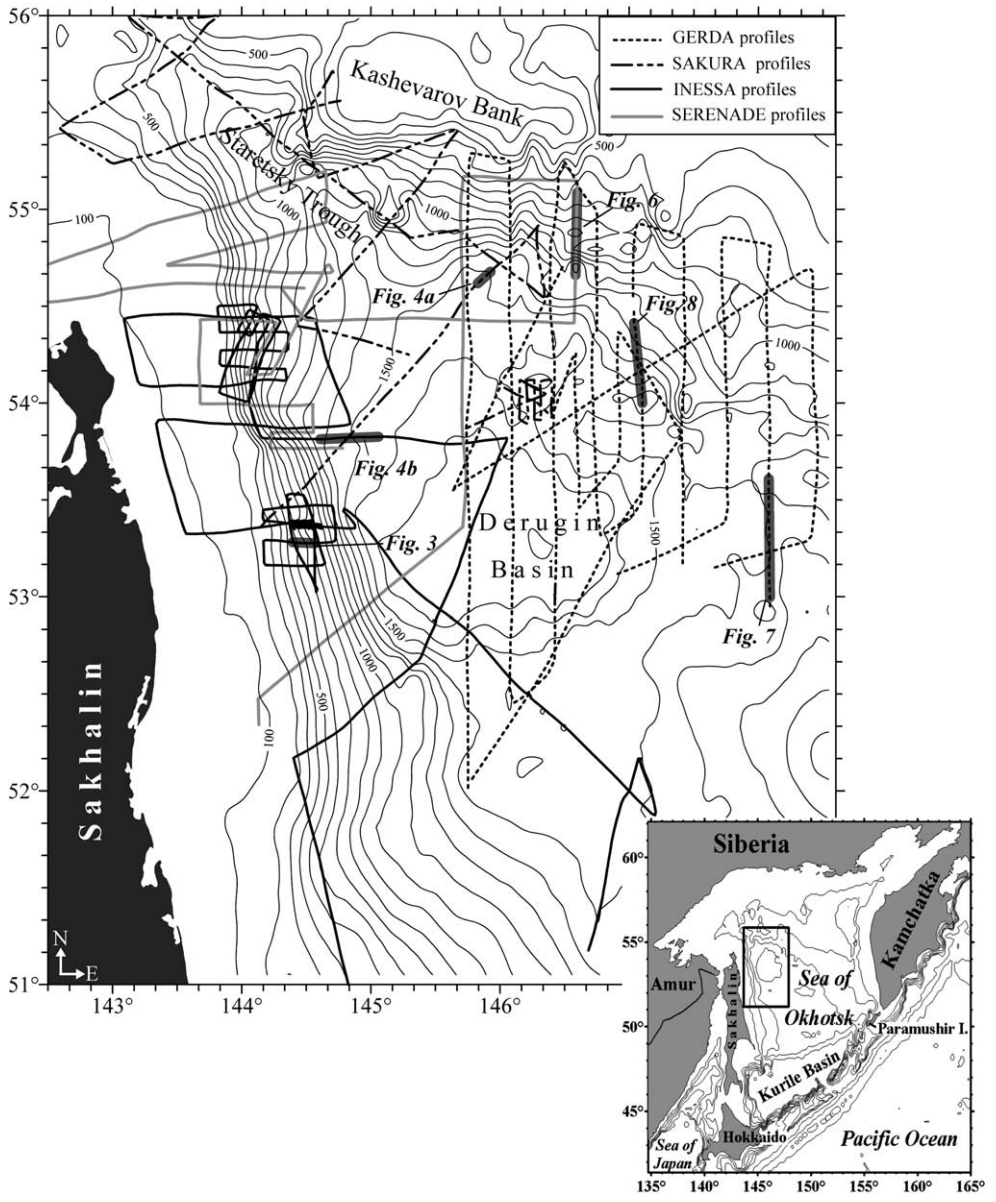

Fig. 1. Seismic profiles obtained within the KOMEX project in the northwestern Sea of Okhotsk. Profiles presented in later figures are shaded in grey. Inset shows the location of the study area (framed).

Okhotsk Marine Experiment in the Sakhalin and Kurile Areas, in 1999) and cruise 32 of R/V *Professor Gagarinsky* (SERENADE: *Seismo-Stratigraphic Research off Northern Sakhalin and in the Derugin Basin*, in 2001). Two different seismic systems were used: The first comprises a single-channel streamer with an active section of 100 m, and a Russian Impuls-1 air gun (dominant frequencies 40–60 Hz) with a volume of 3 l (GERDA cruise). The second system consisted of a GECO Prakla eight-channel mini-streamer with an active length of 100 m, and two S.S.I. GI guns (dominant frequencies 70–90 Hz) with a total volume of 6.88 l as well as an S.S.I. mini-GI

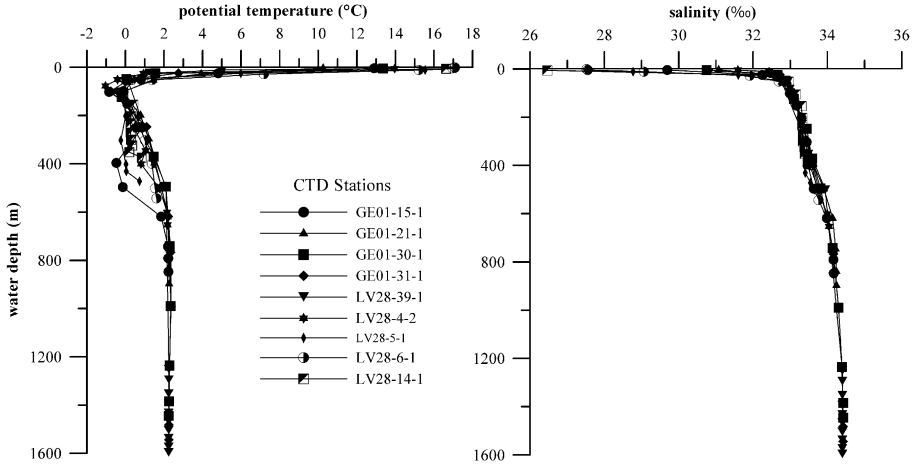

Fig. 2. Vertical salinity and potential temperature as a function of water depth measured at a number of CTD stations in the northwestern Sea of Okhotsk during the KOMEX cruises (Biebow and Hütten, 1999; Biebow et al., 2000).

gun (dominant frequencies 80–170 Hz) with a volume of 1.04 l (the three remaining cruises).

Processing of the multi-channel seismic data included bandpass filtering, spherical divergence correction, signature deconvolution, stacking and time domain F–K migration. Unfortunately, velocity information on the sedimentary column in our study area was not available, either from analysis of our own data, because of the short streamer offset, or from the published literature.

3. Method of deducing heat flow from the depth of the BSR

The two-way travel time to the BSR was read from the seismic sections by picking the onset of the negative swing of the BSR reflection, the phase of which is opposite to that of the seafloor reflection. These travel times were converted to depths (Z_{BSR}) using a constant velocity of 1.7 km/s. For heat flow calculations (H), we assumed a linear temperature gradient and used the simple conductive heat transport relation:

$$H = k\frac{T_{BSR} - T_{bottom}}{Z_{BSR}}$$

where the bottom temperatures (T_{bottom}) are determined from CTD measurements of the KOMEX cruises (Biebow and Hütten, 1999; Biebow et al., 2000) (Fig. 2) and the temperature at the BSR depth (T_{BSR}) was computed by assuming that the BSR represents the lower boundary of the methane HSZ having a known pressure–temperature relationship (Dickens and Quinby-Hunt, 1994). The measured bottom temperatures below 900 m should be in equilibrium with the sediments because the water mass below this depth is regarded as a more or less stagnant body (Freeland et al., 1998) with a consistent temperature of about 2°C. Analyses of gas hydrates from seafloor samples obtained by Cranston et al. (1994) ($CH_4 \approx 97\%$ and $CO_2 \approx 2\%$, 30 ppmv ethane, 15 ppmv propane, 5 ppmv *n*-butane and 2 ppmv *I*-butane) and Obzhirov et al. (2000) ($CH_4 \approx 98$–99% and $CO_2 \approx 1\%$) at the northeastern continental margin of Sakhalin show that methane is the dominant gas. The isotopic composition points to a biogenic origin of the gas hydrates (Cranston et al., 1994). Moreover, the effect of local salinity variations on methane stability conditions in seawater was taken into account using measured CTD bottom water salinities (Fig. 2). For the heat flow calculations (H), the pressure at the BSR depth was assumed to be lithostatic and the average density of the sediments above the BSR was estimated to be 1.7 g/cm^3. To convert the geothermal gradient into heat flow, an average conductivity (k) of 0.92 W m^{-1} K^{-1} was applied. Density, P-wave velocity and conductivity are for

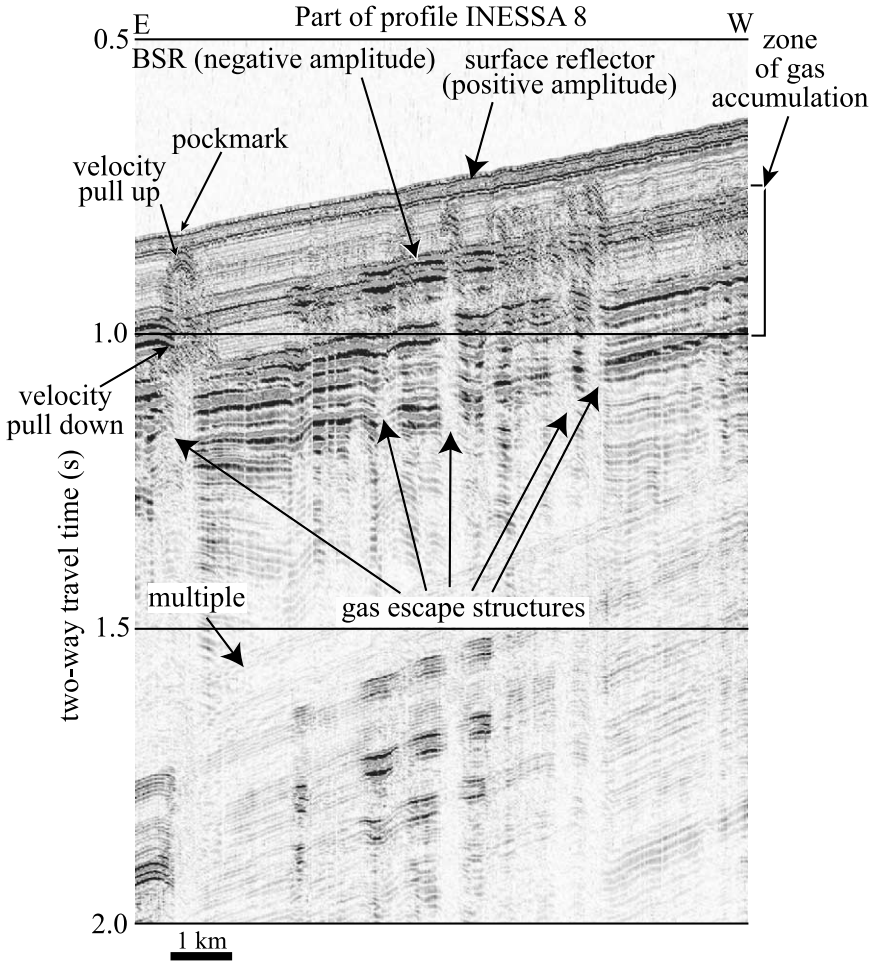

Fig. 3. Part of profile 8 (INESSA) showing gas escape structures and a prominent BSR. See Fig. 1 for profile location.

the upper 700 m of diatomaceous silty clay and diatom ooze at sites 190, 191 and 192, based on borehole logging during DSDP Leg 19 in the Bering Sea (Creager et al., 1973). Analyses of sediment cores of the KOMEX cruises show that the lithology in the study area is comparable to that at the DSDP sites, although here the dominance of fluvial input is absent. Changes in conductivity at the ODP sites are mainly due to variations in the content of clay, diatom ooze, ice-rafted detritus and volcanic ash in the sediments and do not increase systematically with depth. Because lithological information down to the observed BSR depths is lacking, an average conductivity value for the whole sedimentary column was assumed.

3.1. Estimation of error

For the computation of heat flow from BSR depth, the following uncertainties have to be taken into account (percentages represent heat flow errors): (a) inaccuracies in salinity determinations (±0.1‰) and picking error of the BSR (±5 ms). These can be considered negligible; (b) uncertainties in the measured bottom water temperature (±0.05–0.5°C depending on the location). The temperature is nearly constant at depths below 600 m, while its associated error increases at shallower depths because of bottom currents. Here, this relative error leads to a maximum heat flow error of 6%; (c) a possible deviation of ±200 m/s

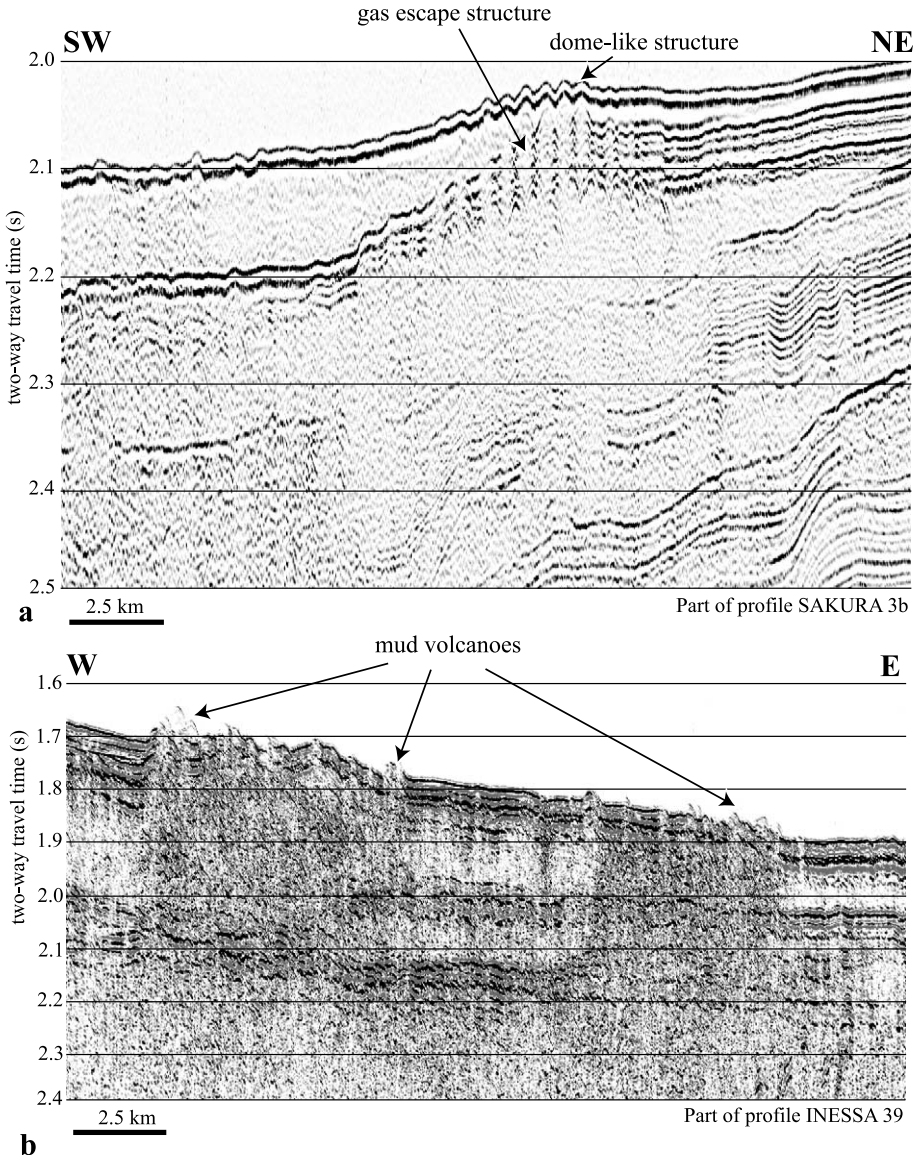

Fig. 4. Parts of seismic profiles (a) 3 (SAKURA) and (b) 39 (INESSA) showing examples of mud volcanoes and gas escape structures. See Fig. 1 for profile locations.

from the average velocity of 1700 m/s used for the determination of the BSR depth leads to an error of approximately 8%; (d) the error in the thermal conductivity used is estimated to be of the order of ± 0.1 W m^{-1} K^{-1}. This results in an error of 11%; (e) density variations of ± 0.2 g/cm^3 account for an error of 2%. The cumulative error in the different parameters gives uncertainties in the uncorrected heat flow of approximately 27%. An additional source of error is suggested by the observed discrepancy between the inferred BSR temperatures and those derived from in situ measurements (borehole logging), as reported by Ruppel (1997) and Wood and Ruppel (2000) for the Blake Ridge. Also, at the ODP sites, the measured surface heat flow values extrapolated to the BSR

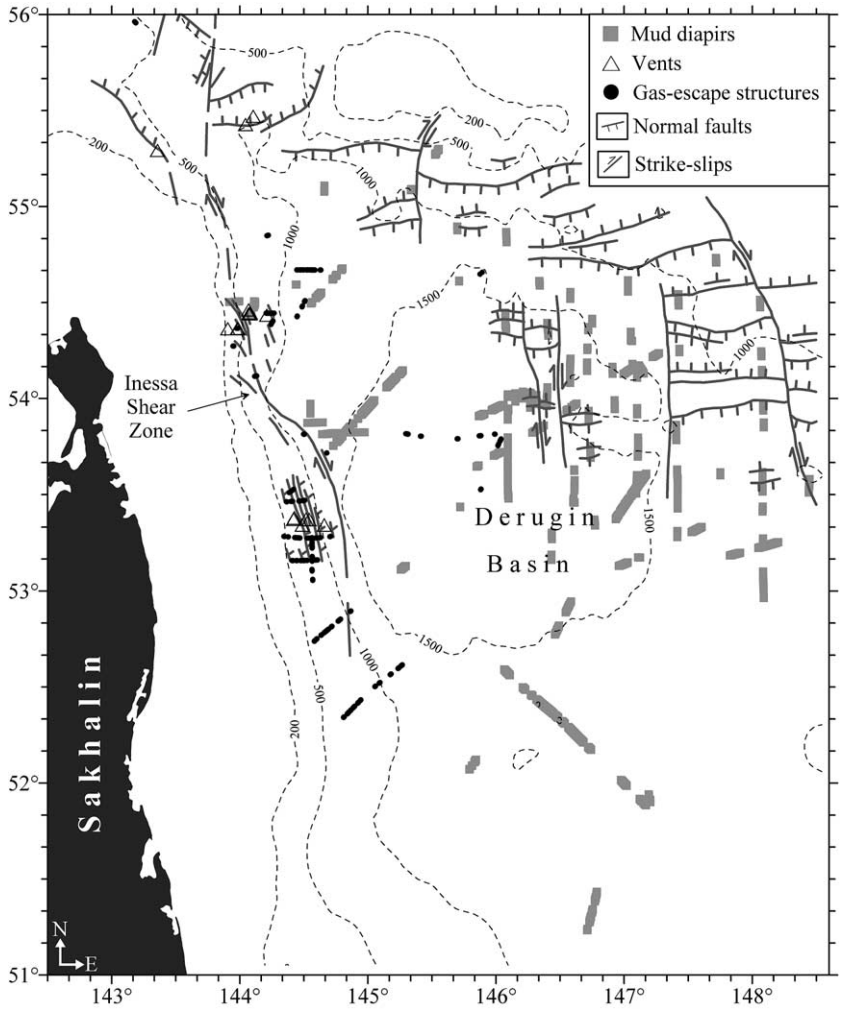

Fig. 5. Map with locations of gas escape structures, vents and mud diapirs as well as the regional fault pattern mapped in the study area. See text for further explanations.

depth are generally lower than the in situ data. The reason for this remains speculative and in our study, this error source has not been considered.

4. Results and discussion

4.1. Gas escape structures, mud diapirism and venting

Gas escape structures, mud diapirs and fluid venting sites have been mapped seismically in the Sea of Okhotsk. In this paper, we will focus on its northwestern part. This area is dominated by the Derugin Basin (Fig. 1), a rift basin probably of Cretaceous to Lower Palaeocene age (Gnibidenko, 1985). Its sedimentary cover thickens from east to west, where it reaches >4 km in places (Worrall et al., 1996).

Gas escape structures characteristically penetrate the sedimentary column nearly vertically and represent a zone of acoustic masking where the original stratification is wiped out (Roberts and Carney, 1997; Bouriak and Akhmetjanov, 1998; Mienert et al., 1998) (Fig. 3). In most cases, these zones are narrow (200–300 m in dimension).

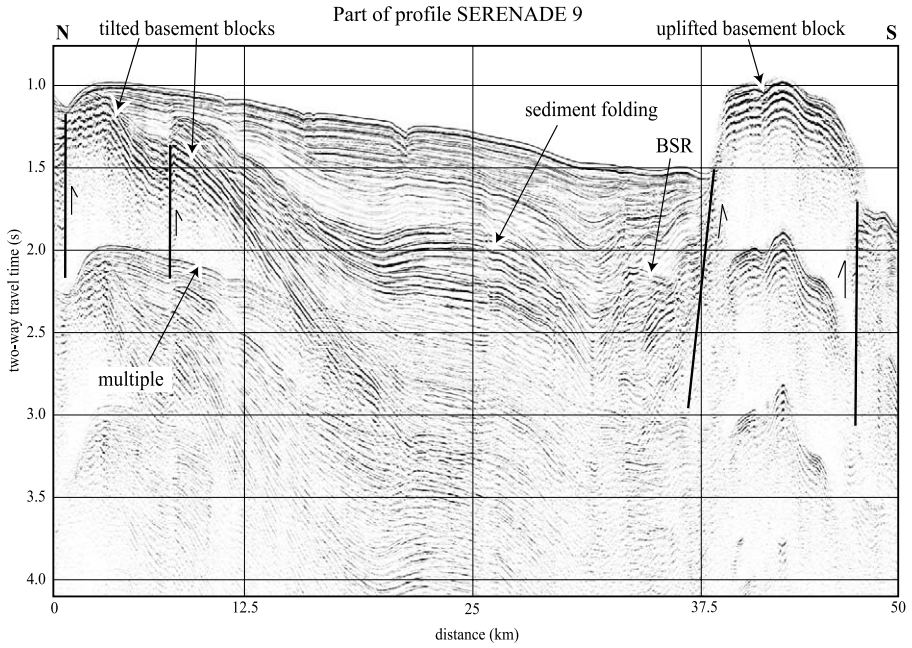

Fig. 6. Part of seismic profile 9 (SERENADE) showing tilted basement blocks and sediment folding. See Fig. 1 for profile location.

They are broader at their base and taper to the top. When they reach the seafloor, they may be associated either with pockmarks or dome-like structures (Figs. 3 and 4a). Fig. 5 shows the distribution of gas escape structures and vents at the seafloor in the northwestern Sea of Okhotsk. The gas escape structures related to seeps show generally a pull-down and occasionally a pull-up reflection pattern as well as an increase in amplitude near the seafloor (Fig. 3). Gas within the sediments significantly decreases the seismic velocities of the P-waves, which leads to pull-down of the reflectors in the contact area of the zone of gas ascent (Fig. 3). The zone itself shows acoustic masking due to the gas content. A pull-up of the reflectors points to a seismic velocity increase which may be due to gas hydrate cementation or authigenic carbonate precipitation near the surface as observed by Derkachev et al. (2000). The BSR amplitude varies laterally, increasing significantly where the conduits break through the BGHSZ (Fig. 3). The same is true of the sediments below the BGHSZ adjacent to the conduits. This may be due to lateral migration of gas in the escape structures into the surrounding permeable layers where it accumulates, thereby increasing the impedance contrast significantly. This process may start at depths where the solubility of gas in the ascending water is considerably reduced as a result of decreasing pressure and temperature. The majority of the gas escape structures and vents are located on the northern Sakhalin continental margin. We attribute this distribution pattern to the regional tectonic regime, which is marked by the prominent, N–S striking, active, dextral Inessa Shear Zone (Baranov et al., 2002) (Fig. 5). The faults of this zone are generally steep and their fault planes act as conduits for fluids. The shear zone is also associated with a higher heat flow (see Section 4.3). A detailed discussion of the tectonic regime is beyond the scope of this paper.

Mud diapirism is widespread in the northwestern Sea of Okhotsk (Fig. 5). It is confined largely to the Derugin Basin, but is also found on the North Okhotsk and northern Sakhalin continental margins. Only occasionally do mud diapirs flank basement uplifts. Previous studies have at-

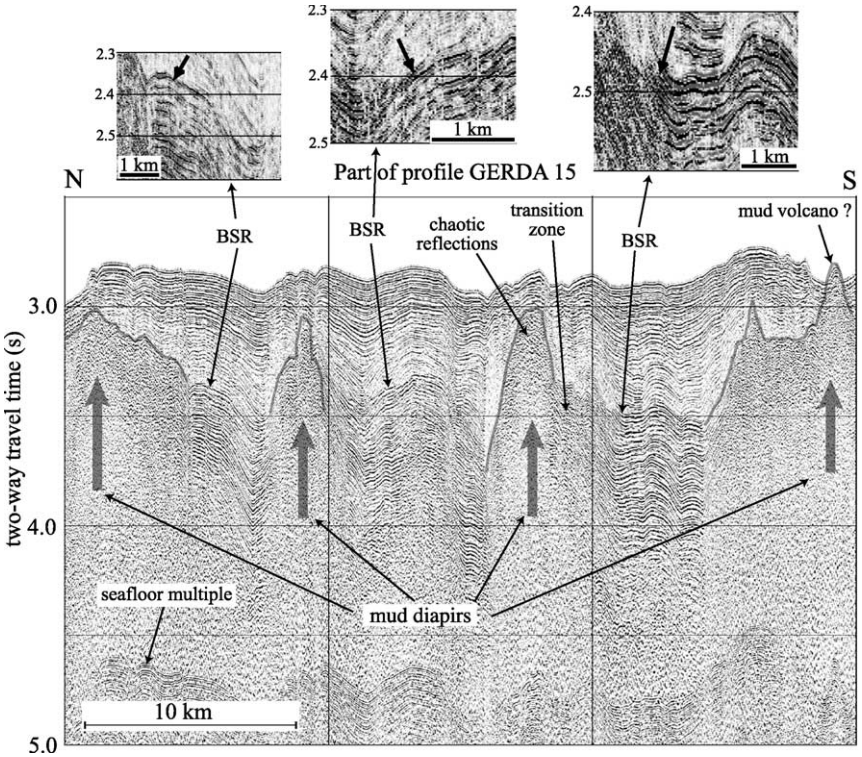

Fig. 7. Part of seismic profile 15 (GERDA) showing several mud diapirs and a possible mud volcano as well as a BSR. See Fig. 1 for profile location.

tributed anticlinal and horst-like structures in the Derugin Basin to uplifted basement blocks or volcanic edifices (Savostin et al., 1983; Gnibidenko, 1985, 1990; Worrall et al., 1996). Our seismic data document the occurrence (especially in the NE basin) of basement blocks (Fig. 6), which correlate well with positive gravity anomalies (altimetric data from the Geosat and ERS 1 satellites, Sandwell and Smith, 1997). Mud diapirism-related structures, on the other hand, are associated with negative anomalies. Most of the interpreted basement blocks which outcrop at the seafloor have been verified by dredging, while several of our mapped mud diapirs dredged in the framework of the KOMEX project yielded soft sediments and dropstones.

Seismically, mud diapirs are characterised by chaotic reflections which have higher amplitudes at their rims than at the centre (Fig. 7). In places, the original layering is preserved within the body of the mud structures. The seismic pattern of the transition zone to the nearby stratified sediments consists of both layered and chaotic reflections. The internal seismic transparency of the mud diapirs could be a result of mud ascent, which leaves the diapirs internally homogeneous and hence unreflective. Alternatively, the layering could be masked by gas (Hampton and Anderson, 1974; Minshull and White, 1989). Even in low concentrations, gas in pore fluids causes a distinct reduction in seismic velocity while leaving the density relatively unaffected. Most of the mud diapirs give rise to doming of the overlying strata, but only a few penetrate the seafloor to become mud volcanoes (Figs. 4b and 7). The majority rise from below the BSR, thereby interrupting its continuity. In places diapirs are conical in shape, with heights of a few metres to more than 500 m and a width at their base of 1–5 km. However, ridge-like structures also occur with rough mound-like tops of more than 10 km in width (Fig. 7).

The driving mechanism for mud diapirism is

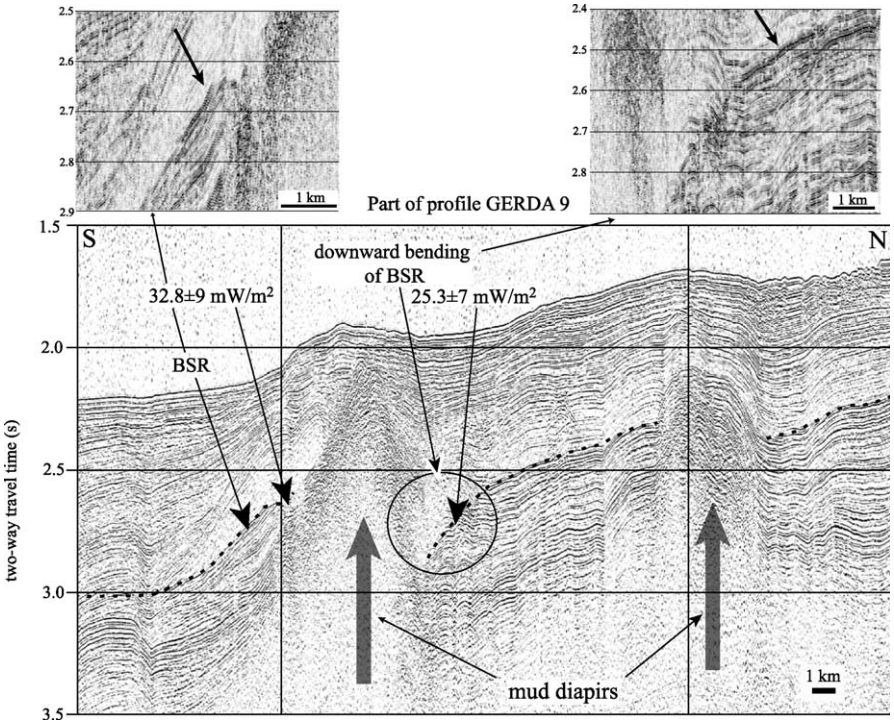

Fig. 8. Part of seismic profile 9 (GERDA) illustrating a mud diapir with shoaling of the BSR at its southern flank and deepening at its northern flank (circle). Also shown are computed heat flow values derived from the BSR depth. See text for further explanations and Fig. 1 for profile location.

the existence of a source layer with a density lower than that of the overlying strata and a viscosity sufficiently low to enable upward flow or creep. This is usually the case if salt underlies denser sedimentary layers, but is true also when over-pressuring occurs in mud and mudstones (Braunstein and O'Brien, 1968). Over-pressuring can be generated by: (1) an increase in compressive stress (i.e. a reduction in pore space) triggered by disequilibrium compaction and tectonic compression; (2) a fluid volume change caused by temperature increase (aquathermal pressuring), diagenesis, hydrocarbon generation, and cracking to gas; and (3) fluid movement as well as processes related to density differences between fluid and gas caused by a hydraulic (potentiometric) head, osmosis, and buoyancy (Osborne and Swarbrick, 1997).

In the study area, conditions for over-pressuring are met by the dominance of rapidly accumulated diatomaceous clays especially during interglacial times (Gorbarenko et al., 1990; Astakhov et al., 2000; Shiga and Koizumi, 2000) (which have been compacted during burial), and the presence of free gas below the BGHSZ. Whether the stratigraphic layers below the BGHSZ or the gas hydrate in the HSZ serve as a seal for the rising fluids or gas is unknown. That gas hydrates function as an effective seal appears unlikely because gas migration through the BGHSZ and within the HSZ has been reported (Taylor et al., 2000; Gorman et al., 2002). Diapirism triggering may be due to vertical hydraulic fracturing, when the pore-fluid pressure exceeds the lithostatic pressure (Dimitrov, 2002), or it may be tectonic, which we consider most probable. Folding of and faulting in the sediments observed in our seismic profiles suggest the occurrence of high compressional stress (Fig. 6). This may have led locally to disruption of the impermeable layer, especially on top of anticlinal structures and along fault planes. The mud ascends until the internal pressure and

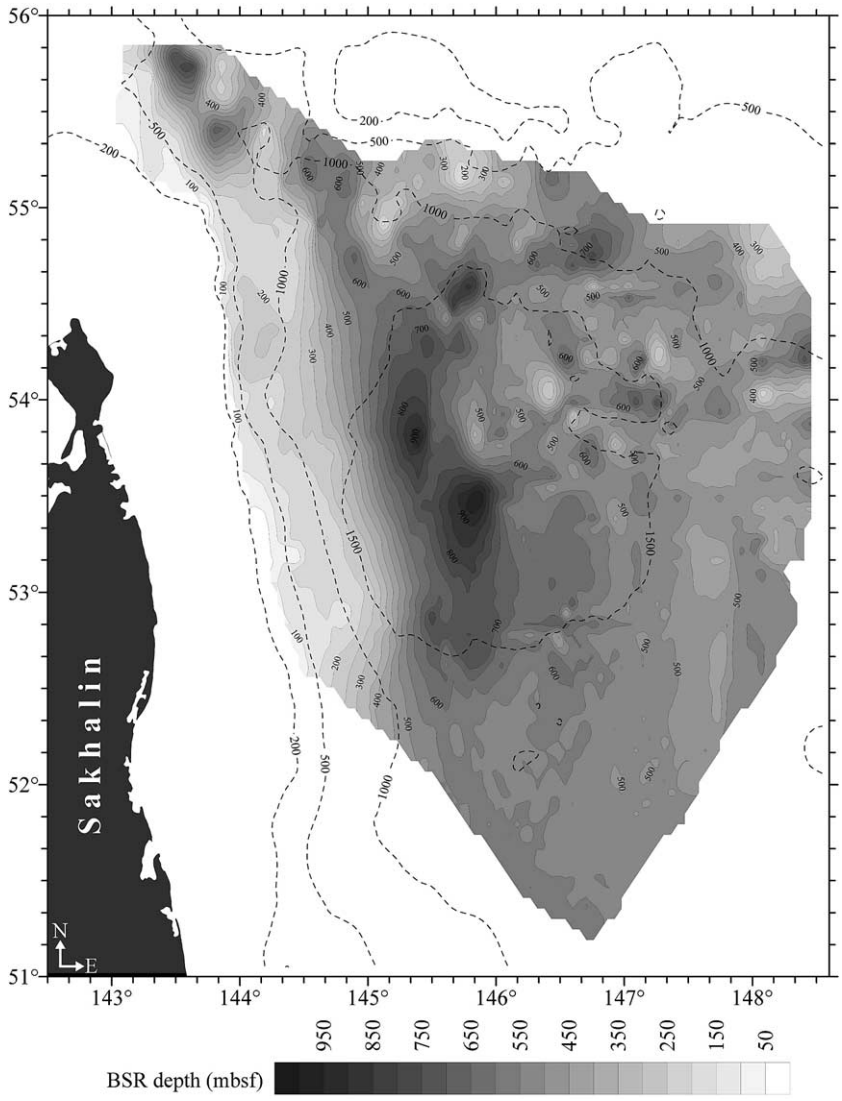

Fig. 9. Map showing the distribution of the depth of the BSR in m below seafloor (continuous lines) and the water depth (dashed lines).

density are in equilibrium with their ambient values.

Diapirism in association with gas hydrate occurrence is well-known from the Blake Ridge (Dillon et al., 1983; Taylor et al., 2000), the Fairway Basin (Auzende et al., 2000) and the Vøring Plateau (Bouriak et al., 2000). In our study area, shoaling as well as deepening of the BSR occurs adjacent to the diapirs. An example is shown on GERDA profile 9 (Fig. 8). Here, the BSR deepens distinctly on the northern flank of the southern diapir, leading to a much lower calculated heat flow (25.3 ± 7 mW m^{-2}) compared to that (32.8 ± 9 mW m^{-2}) on the southern flank, where the BSR is shallower. We attribute this down-bending of the BSR to a significant increase in pressure associated with the injection of gas and fluids into the adjacent sediments (transparent zone on the northern flank; Fig. 8, circle). We infer that expansion of gas here has increased

the in situ pressure and, because the expansion is an endothermic process, lowered the surrounding temperature. These combined effects shift the BGHSZ increasingly downward towards the rim of the mud diapir. Gas expansion during upward mud intrusion has also been reported by Van Rensbergen et al. (1999) for diapirs offshore Brunei Darussalam. In contrast, on its southern flank, the diapir is sealed by the convex sedimentary strata (Fig. 8). Here, conductive heat flow from the interior of the mud diapir may have raised the BGHSZ in the contact zone.

Another phenomenon which seems to be closely related to mud diapirism is barite and calcite mineralisation associated with cold seeps as described by by Greinert et al. (2002) for the deep Derugin Basin. They interpret the region where these mineralisations occur at the seafloor as a tectonic horst, but our seismic lines suggest an uplifted and tectonised mud diapir, whose bounding fault planes provide pathways for fluid migration.

4.2. Gas hydrate occurrence

The depth distribution of the BSR in the northwestern Sea of Okhotsk is shown in Fig. 9. The BSR can be traced from c. 50 m subbottom on the upper continental slope to more than 800 m below the seafloor in the Derugin Basin. Characteristic for the BSR in our study area is an overlying broad zone in which the amplitudes of the reflectors are significantly reduced (Figs. 6–8). The average thickness of this zone is c. 180 m in the Derugin Basin. On the Blake Ridge, a similar zone of low reflectivity has been ascribed to lithologic homogeneity of the sediments (Holbrook et al., 1996; Wood and Gettrust, 2001). We do not consider this attribution applicable to the Sea of Okhotsk because the transparent zone here occurs irrespective of the depo-environment and must therefore be independent of sedimentation processes. We suggest that the finely dispersed gas hydrate which replaced water in the pore space of the sediments above the BGHSZ but is still in the HSZ has sharply reduced the acoustic impedance between the adjacent layers and with it the reflection coefficient. The hydrates accumulate preferably in the pores of the less dense material

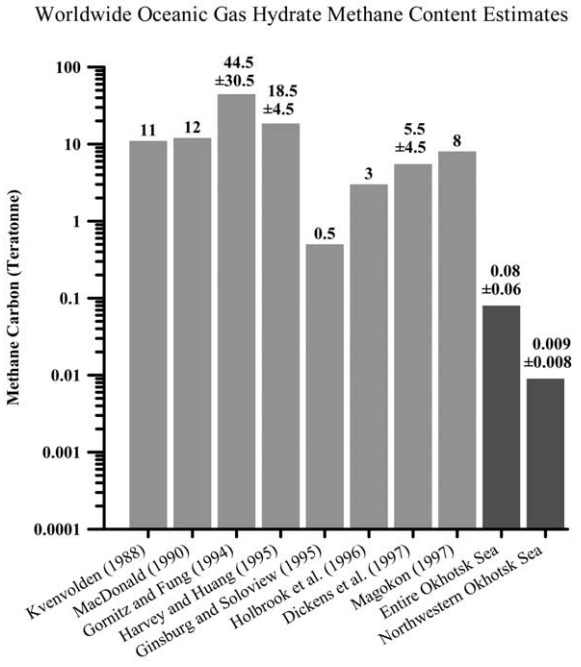

Fig. 10. Histogram of estimates of methane carbon in worldwide gas hydrate occurrences (grey bars). Results of this study are shown in dark grey (modified after Kvenvolden and Lorenson, 2001; data from: Kvenvolden, 1988; MacDonald, 1990; Gornitz and Fung, 1994; Harvey and Huang, 1995; Ginsburg and Soloview, 1995; Holbrook et al., 1996; Dickens et al., 1997; Magokon, 1997).

(diatomaceous ooze; as shown for the Blake Ridge by Kraemer et al., 2000) as nn-contact cement (nn-contact cement model of Ecker et al., 1998), thereby reducing its density contrast to the denser material (e.g. silty clay) without significantly increasing V_p. The accumulation may have taken place during the pressure-controlled gradual downward shift of the BGHSZ in the course of sedimentation and basin subsidence, when the sediment and water loads increase.

We shall now attempt an order-of-magnitude estimate of the amount of gas preserved in the form of gas hydrate at the base of the stability zone. Due to the lack of V_p and V_s information our calculation is based on data from other regions. On the Blake Ridge, a sediment drift composed of homogeneous nannofossil-rich clays with finely disseminated gas hydrates occupies 5–7% of the pore space between 200 and 450 m below sea

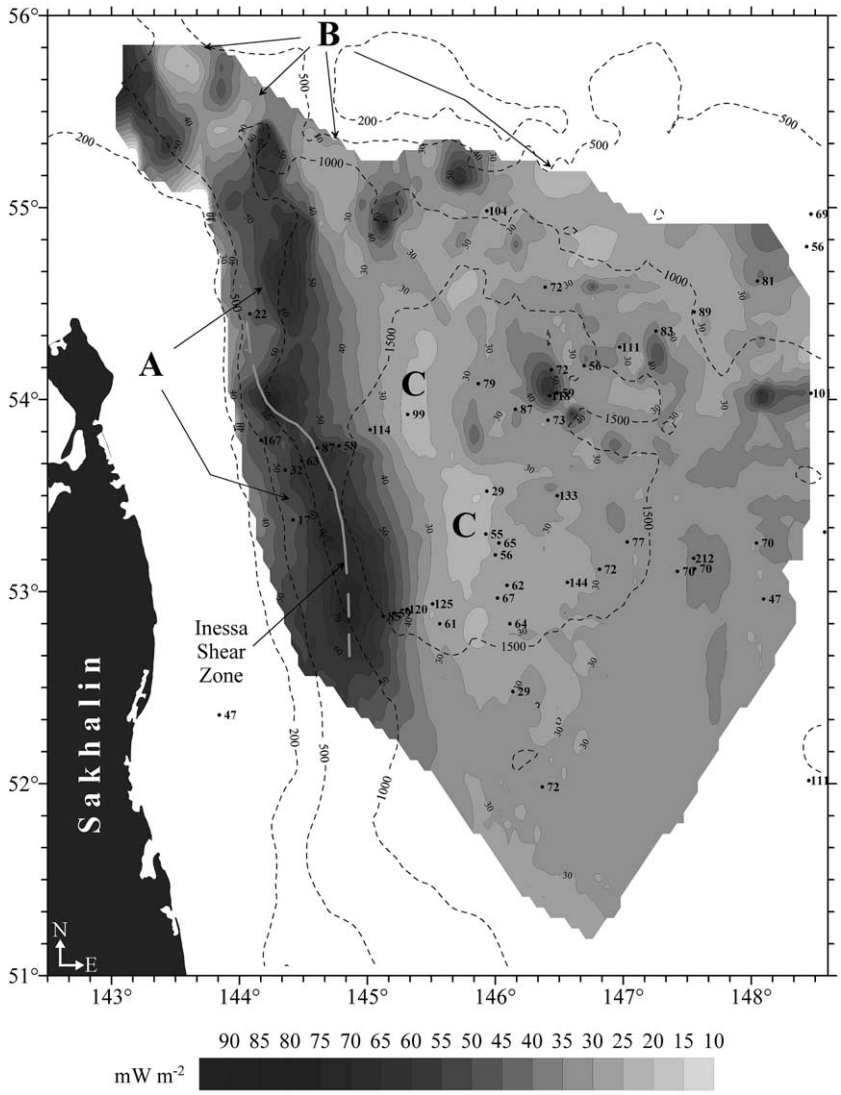

Fig. 11. Map showing the distribution of heat flow in mW m^{-2} (continuous lines), water depth (dashed lines) and the Inessa Shear Zone. (A) Area of tectonic activity indicated by gas escape structures, fluid venting and high heat flow values; (B) area of drift sedimentation characterised by high sedimentation rates and low heat flow values; (C) area of mass wasting deposits marked by rapid sedimentation and very low heat flow values. In addition, measured surface heat flow values are given.

level (Holbrook et al., 1996; Paull et al., 1996, 1998). The free gas in a zone up to 200 m below the BGHZ is estimated to occupy 1% of porosity. For the Storegga Slide area (Norwegian slope), Bouriak et al. (2000) suggest a hydrate concentration of 5–10% of the pore volume. Hovland et al. (1997) estimate the amount of hydrate residing in the sediments of the Niger delta front (continental margin of West Africa) at 3% by volume and free gas below the BSR at 5% by volume. Data from convergent margin settings are not applicable to our study area because they show much higher fluid expulsion rates, which result in significant higher hydrate and free gas concentrations.

For our estimates, we adopted for the gas hydrate-bearing sediments in the northwestern Sea

of Okhotsk an average thickness of 100–200 m (thickness of the gas hydrate-saturated low-reflectivity zone above the BSR), an average sediment porosity of 50–70% (DSDP Leg 19, Creager et al., 1973), and an average hydrate-filled pore volume of 3–10%. Furthermore, to estimate the amount of free gas beneath the BSR, we assumed an average thickness of the gas-enriched sediments of 100–200 m, and an average gas-filled pore volume of 1–5%. We also assumed that gas hydrates are always present above the BSR. Our seismic profiles suggest that a BSR occurs in about 90% of the study area in the northwestern Sea of Okhotsk (c. 13 500 km^2; Table 1). This yields estimates of $50 \pm 43 \times 10^9$ m^3 for the amount of free gas below the BSR and $17 \pm 14 \times 10^{12}$ m^3 for the volume of gas associated with gas hydrates above the BSR (1 m^3 gas hydrate = 164 m^3 gas at STP). The total is therefore approximately $17 \pm 14 \times 10^{12}$ m^3. To extrapolate to the entire Sea of Okhotsk, we note that a BSR was observed in the water depth range of 250 to over 3000 m, including the Kurile Basin. This implies an area of about 145 200 km^2, of which c. 20% is BSR-free, namely where the basement crops out at the seafloor. Thus, the area in which gas hydrates occur in the Sea of Okhotsk is c. 116 000 km^2, yielding $43 \pm 37 \times 10^{10}$ m^3 free gas and $15 \pm 12 \times 10^{13}$ m^3 gas from gas hydrates (Table 1). The total methane volume in the Sea of Okhotsk is therefore of the order of $15 \pm 12 \times 10^{13}$ m^3. Fig. 10 shows a comparison of the computed values (Table 1) for the study area with estimates of the global reservoir of methane carbon associated with gas hydrates from the literature. It suggests that the Sea of Okhotsk represents c. 0.8% of the mean global reservoir of 10 teratonnes methane carbon (Kvenvolden and Lorenson, 2001).

4.3. Heat flow variations vs tectonic regime

Where heat flow measurements are not available, the local conductive heat flow can be estimated from the BSR depth (Yamano et al., 1982; Hyndman et al., 1992; Townend, 1997; Kaul et al., 2000). Even where heat flow has been measured directly, such estimates are still valuable. This is because heat flow probes penetrate only a few metres of the sedimentary column and are sensitive to lateral advection and local topographic effects, so that the measured geothermal gradient is subject to error and must be extrapolated to greater depths. Fig. 11 shows the heat flow distribution derived from BSR depths in the study area. The average heat flow is about 30 ± 8 mW m^{-2}; values exceeding 85 ± 23 mW m^{-2} are found only on the northeastern Sakhalin continental margin, where the isolines show a pronounced N–S elongation (Fig. 11A). Responsible for the higher heat flow are tectonic movements along the N–S trending dextral Inessa Shear Zone (Fig. 11, only the trend of the master fault is shown) in which faults reach the seafloor in places. The trace of this shear system is characterised by a restraining bend at the continental slope off northeastern Sakhalin (Figs. 5 and 11), which is also reflected in the heat flow pattern (Fig. 11). Likewise many of the gas escape structures and vents are located on the faults of this zone (Fig. 5). They act as pathways for warm fluids ascending to the seafloor and heating the surrounding sediments, which accounts for the BSR rise. In the Derugin Basin, the heat flow is more or less uniform. Higher values are associated with basement horsts where uplifted blocks presumably lead to higher thermal gradients and to a rise in the gas hydrate stability boundary. Regions of

Table 1
Volume of methane gas associated with gas hydrates and free gas below the BGHSZ in the KOMEX study area

	Northwestern Sea of Okhotsk	Entire Sea of Okhotsk
Area of gas hydrate occurrence (km^2)	13 500	116 000
Methane confined to gas hydrate layer (m^3)	$17 \pm 14 \times 10^{12}$	$15 \pm 12 \times 10^{13}$
Free gas below gas hydrate layer (m^3)	$50 \pm 43 \times 10^9$	$43 \pm 37 \times 10^{10}$
Free gas and gas from hydrates (m^3)	$17 \pm 14 \times 10^{12}$	$15 \pm 12 \times 10^{13}$
Methane carbon (teratonnes)	0.009 ± 0.008	0.08 ± 0.06

low heat flow marked by B and C in Fig. 11 are associated with high sedimentation rates due to drift sedimentation and mass wasting (Wong et al., in press) respectively. Compared to the computed values, measured heat flow values at the continental margin are of about the same magnitude but are generally higher in the Derugin Basin (Fig. 11). However, they have a large scatter (29.3–212 mW m^{-2}, mean 85.1 mW m^{-2}). The discrepancy between the measured and computed heat flows in the Derugin Basin might be partially caused by the effect of sedimentation. Particles which settle onto the seafloor have the temperature of the water column and a part of the rising conductive heat has to be used to heat the newly accumulated sediment which in effect reduces the conductive heat flow at the surface. A correction of the estimated heat flow using the method of Jaeger (1965) leads to 3% or 20% higher heat flow for a mean sedimentation rate of 3.8 cm/kyr or 1 m/kyr (Gorbarenko et al., 1990; Botsul et al., 1999; Astakhov et al., 2000) respectively. A second explanation for the deviation could be lateral advection because many of the heat flow stations close to our profiles are located around mud diapirs and are probably affected by fluid circulations in the tectonised sedimentary cover on top of the diapirs.

5. Conclusions

Our seismic studies within the framework of the KOMEX project show that there is a widespread occurrence of free gas or gas hydrates in the northwestern Sea of Okhotsk. They are documented seismically by gas escape structures, acoustic blanking and by a BSR.

Gas/fluid escape structures and gas seeps are located mainly on the northern Sakhalin continental margin. Here, they are associated with dextral transpressional movements along the N–S trending Inessa Shear Zone. Mud diapirism is concentrated in the Derugin Basin, where it originates at or below the BGHSZ and in places penetrates the sedimentary column to form mud volcanoes at the seafloor. We attribute this diapirism to the compressional tectonic regime in the Derugin Basin and to free gas and fluids beneath the BGHSZ.

The total amount of gas bound to gas hydrates in the HSZ and free gas beneath is approximately $15 \pm 12 \times 10^{13}$ m^3 for the entire Sea of Okhotsk (about 0.8% of the global amount of methane carbon from hydrates) and $17 \pm 14 \times 10^{12}$ m^3 for its northwestern part. Heat flow computed from the BSR depth averages 30 ± 8 mW m^{-2}. Values of 80 ± 23 mW m^{-2} and higher are related to transpressional tectonic movements along the shear zone off Sakhalin and basement uplift in the Derugin Basin; lower values are associated with areas of high sedimentation rates. A correction of the estimated heat flow for the effect of sedimentation using the method of Jaeger (1965) leads to 3% or 20% higher heat flow for a mean sedimentation rate of 3.8 cm/kyr or 1 m/kyr, respectively.

This study shows that the Sea of Okhotsk must be regarded as a large reservoir for methane and associated gases. However, finely disseminated gas hydrates in the sediments are at present not of economical interest (Laherrere, 2000). Any significant environmental changes such as global warming may destabilise the hydrates and lead to a major release of methane into the atmosphere. Gas hydrates could have been involved in the destabilisation of the slope sediments in the northern Okhotsk Sea (Wong et al., in press) and near Paramushir Island (Gaedicke et al., 1997).

Acknowledgements

We gratefully acknowledge the unfailing help of the captains, officers, crew and in particular the scientific parties of the R/V *Professor Gagarinsky* and R/V *Akademik Lavrentyev* during the four Sea of Okhotsk cruises reported here. Special thanks are due to our Russian colleagues Boris Baranov, Karina Dozorova and Boris Karp for a fruitful cooperation and stimulating discussions. We also thank Christoph Gaedicke and Jürgen Mienert for critically reviewing this manuscript. This work is carried out within the framework of the German–Russian cooperative project KOMEX, which is funded by the German Federal

Ministry of Education and Research (Projects 03G0535D and 03G0568B) and by the Russian Ministry of Industry and Science.

References

Astakhov, A., Botsul, A., Biebow, N., Derkachev, A., Fessler, S., Gobarenko, S., Kaiser, A., Nikolayeva, R., Tiedemann, R., Werner, R., 2000. Paleoceanography and sedimentology. In: Biebow, N., Lüdmann, T., Karp, B.Ya., Kulinich, R. (Eds.), KOMEX: Kurile-Sea of Okhotsk Marine Experiment. Cruise Reports: KOMEX V and KOMEX VI, R/V Professor Gagarinsky Cruise 26 and M/V Marshal Gelovany Cruise 1. GEOMAR Report 88, Kiel, pp. 189–209.

Auzende, J.M., van de Beuque, S., Dickens, G., François, C., Lavoy, Y., Voutay, O., Exon, N., 2000. Deep sea diapirs and bottom simulating reflector in Fairway Basin (SW Pacific). Mar. Geophys. Res. 21, 579–587.

Baranov, B.V., Karp, B.Ya., Karnaukh, V., 2002. Western Okhotsk Sea: multifarious tectonic structure. In: Lüdmann, T., Baranov, B.V., Karp, B.Ya. (Eds.), KOMEX: Kurile-Sea of Okhotsk Marine Experiment. Cruise Report R/V Professor Gagarinsky Cruise 32. SERENADE: Seismo-Stratigraphic Research off Northern Sakhalin and in the Derugin Basin. GEOMAR Report 105, Kiel, pp. 32–39.

Basov, E.I., Gaedicke, C., van Weering, T.C.E., Baranov, B.V., Lelikov, E.P., Obzhirov, A.I., Belykh, I., 1996. Seismic facies and the specific character of the bottom-simulating reflector on the western margin of Paramushir Island, Sea of Okhotsk. Geo-Mar. Lett. 16, 297–304.

Biebow, N., Hütten, E., 1999. KOMEX: Kurile-Sea of Okhotsk Marine Experiment. Cruise Reports: KOMEX I and KOMEX II, R/V Professor Gagarinsky cruise 22 and R/V Akademik M.A. Lavrentyev cruise 28. GEOMAR Report 82, Kiel, 377 pp.

Biebow, N., Lüdmann, T., Karp, B.Ya., Kulinich, R., 2000. KOMEX: Kurile-Sea of Okhotsk Marine Experiment. Cruise Reports: KOMEX V and KOMEX VI, R/V Professor Gagarinsky cruise 26 and M/V Marshal Gelovany cruise 1. GEOMAR Report 88, Kiel, 296 pp.

Botsul, A., Biebow, N., Derkachev, A., Gorbarenko, S., Kaiser, A., Nürnberg, D., Terekhov, Y., Tiedemann, R., Werner, R., 1999. Paleoceanography and sedimentology in the Sea of Okhotsk. In: Biebow, N., Hütten, E. (Eds.), KOMEX: Kurile-Sea of Okhotsk Marine Experiment. Cruise Reports: KOMEX I and KOMEX II, R/V Professor Gagarinsky Cruise 22 and R/V Akademik M.A. Lavrentyev cruise 28. GEOMAR Report 82, Kiel, pp. 148–177.

Bouriak, S.V., Akhmetjanov, A.M., 1998. Origin of gas hydrate accumulations on the continental slope of the Crimea from geophysical studies. In: Henriet, J.-P., Mienert, J. (Eds.), Gas Hydrates: Relevance to World Margin Stability and Climate Change. Geol. Soc. Lond. Spec. Publ. 137, pp. 275–291.

Bouriak, S., Vanneste, M., Saoutkine, A., 2000. Inferred gas hydrates and clay diapirs near the Storegga Slide on the southern edge of the Vøring Plateau, offshore Norway. Mar. Geol. 163, 125–148.

Braunstein, J., O'Brien, G.D., 1968. Diapirism and Diapirs. Am. Assoc. Pet. Geol. Mem. 8, 444 pp.

Cranston, R.E., Ginsburg, G.D., Soloviev, V.A., Lorenson, T.D., 1994. Gas venting and hydrate deposits in the Sea of Okhotsk. Bull. Geol. Soc. Denmark 41, 80–85.

Creager, J.S., Scholl, D.W. and the DSDP Leg 19 Shipboard Scientific Party, 1973. Initial Reports of the Deep Sea Drilling Project Leg 19, Washington, DC, 913 pp.

Derkachev, A., Nikolayeva, N., Botsul, A., Greinert, J., 2000. Authigenic minerals and sediments of the Sakhalin Island slope. In: Biebow, N., Lüdmann, T., Karp, B., Kulinich, R. (Eds.), KOMEX: Kurile-Sea of Okhotsk Marine Experiment. Cruise Reports: KOMEX V and KOMEX VI, R/V Professor Gagarinsky Cruise 26 and M/V Marshal Gelovany Cruise 1. GEOMAR Report 88, Kiel, pp. 180–181.

Dickens, G.R., Quinby-Hunt, M.S., 1994. Methane hydrate stability in seawater. Geophy. Res. Lett. 21, 2115–2118.

Dickens, G.R., Paull, C.K., Wallace, P. and the ODP Leg 164 Scientific Party, 1997. Direct measurement of in situ methane quantities in a large gas-hydrate reservoir. Nature 385, 426–428.

Dillon, W.P., Popenoe, P., Grow, J.A., Klitgord, K.D., Swift, B.A., Paull, C.K., Cashman, K., 1983. Growth faulting and salt diapirism: their relationship and control in the Carolina Trough, eastern North America. Stud. Cont. Margin Geol. 34, 21–46.

Dimitrov, L.I., 2002. Mud volcanoes - the most important pathway for degassing deeply buried sediments. Earth-Sci. Rev. 59, 49–76.

Ecker, C., Dvorkin, J., Nur, A., 1998. Sediments with gas hydrates: internal structure from seismic AVO. Geophysics 63, 1659–1669.

Freeland, H.J., Bychkov, A.S., Whitney, F., Taylor, C., Wong, C.S., Yurasov, G.I., 1998. WOCE section P1W in the Sea of Okhotsk 1. Oceanographic data description. J. Geophys. Res. 103, 15613–15623.

Gaedicke, C., Baranov, B.V., Obzhirov, A.I., Lelikov, E.P., Belykh, I.N., Basov, E.I., 1997. Seismic stratigraphy, BSR distribution, and venting of methane-rich fluids west off Paramushir and Onekotan Islands, northern Kuriles. Mar. Geol. 136, 259–276.

Ginsburg, G.D., Soloviev, V.A., 1995. Submarine gas hydrates estimation: theoretical and empirical approaches. Offshore Technology Conference, OTC 7693, vol. 1, pp.513–518.

Gnibidenko, H.S., 1985. The Sea of Okhotsk-Kurile Islands Ridge and Kurile-Kamshatka Trench. In: Nairn, A.E.S., Stehli, F.G., Ueda, S. (Eds.), The Oceanic Basins and Margins, 7A. Plenum Press, New York, pp. 377–418.

Gnibidenko, H.S., 1990. The rift system of the Okhotsk Sea. In: Proc. of the First Int. Conference on Asian Marine Geology (Shanghai, Sept. 7–10, 1988). China Ocean Press, Beijing, pp. 73–81.

Gorbarenko, S.A., 1991. The stratigraphy of the upper Qua-

ternary sediments in the central part of the Sea of Okhotsk and its paleoceanology according to data obtained by the $\delta^{18}O$ and other methods. Oceanology 31, 761–766.

Gorbarenko, S.A., Kovalyukh, N.N., Odinokova, L.Yu., Rybakov, V.F., Tokarchuk, T.N., Shapovalov, V.V., 1990. Upper Quaternary sediments of the Sea of Okhotsk and the reconstruction of paleoceanologic conditions. Geol. Pac. Ocean 6, 309–330.

Gorman, A.R., Holbrook, W.S., Hornbach, M.J., Hackwith, K.L., Lizarralde, D., Pecher, I., 2002. Migration of methane gas through the hydrate stability zone in a low-flux hydrate province. Geology 30, 327–330.

Gornitz, V., Fung, I., 1994. Potential distribution of methane hydrates in the world's ocean. Glob. Biogeochem. Cycl. 8, 335–347.

Greinert, J., Bollwerk, S., Derkachev, A., Bohrmann, G., Suess, E., 2002. Massive barite deposits and carbonate mineralization in the Derugin Basin, Sea of Okhotsk: precipitation processes at cold seep sites. Earth Planet. Sci. Lett. 203, 165–180.

Hampton, L.D., Anderson, A.L., 1974. Acoustics and gas in sediments: Applied Research Laboratories (ARL) experience. In: Kaplan, I.R. (Ed.), Natural Gases in Marine Sediments. Plenum Press, New York, pp. 249–275.

Harvey, L.D.D., Huang, Z., 1995. Evaluation of the potential impact of methane clathrate destabilization on the future global warming. J. Geophys. Res. 1000(D5), 2905–2926.

Holbrook, W.S., Hoskins, H., Wood, W.T., Stephen, R.A., Lizarralde, D., 1996. Methane hydrate and free gas on the Blake Ridge from vertical seismic profiling. Science 273, 1840–1843.

Hovland, M., Gallagher, J.W., Clennell, M.B., Lekvam, K., 1997. Gas hydrate and free gas volumes in marine sediments: example from the Niger Delta front. Mar. Petr. Geol. 14, 245–255.

Hyndman, R.D., Foucher, J.P., Yamano, M., Fisher, A. and Scientific Team of Ocean Drilling Program Leg 131, 1992. Deep sea bottom-simulating-reflectors: calibration of the base of the hydrate stability field as used for heat flow estimates. Earth Planet. Sci. Lett. 109, 289–301.

Hyndman, R.D., Spence, G.D., 1992. A seismic study of methane hydrate marine bottom simulating reflectors. J. Geophys. Res. 97, 6683–6698.

Jaeger, J.C., 1965. Application of the theory of heat conduction to geothermal measurements. In: Lee, W.H.K. (Ed.), Terrestrial Heat Flow. Am. Geophys. Union, Washington, DC, pp. 7–13.

Kaul, N., Rosenberger, A., Villinger, H., 2000. Comparison of measured and BSR-derived heat flow values, Makran accretionary prism, Pakistan. Mar. Geol. 164, 37–51.

Kitani, K., 1973. An oceanographic study of the Sea of Okhotsk particularly in regard to cold waters. Bull. Far Seas Fish. Res. Lab. 9, 45–77.

Kraemer, L.M., Owen, R.M., Dickens, G.R., 2000. Lithology of the upper gas hydrate zone, Blake Outer Ridge: a link between diatoms, porosity, and gas hydrate. In: Paull, C.K., Matsumoto, R., Wallace, P.J., Dillon, W.P. (Eds.), Proceedings of the Ocean Drilling Program, Scientific Results Leg 164. Ocean Drilling Program, College Station, TX, pp. 229–236.

Kvenvolden, K.A., 1988. Methane hydrate - A major reservoir of carbon in shallow water geosphere? Chem. Geol. 71, 41–51.

Kvenvolden, K.A., Lorenson T.D., 2001. The global occurrence of natural gas hydrate. In: Paull C.K., Dillon W.P. (Eds.), Natural Gas Hydrates: Occurrence, Distribution, and Detection. AGU Geophys. Monogr. 124, 3–18.

Laherrere, J., 2000. Oceanic hydrates: more questions than answers. Ener. Explor. Exploit. 18, 349–384.

MacDonald, G.T., 1990. Role of methane clathrates in past and future climates. Clim. Change 16, 247–281.

Magokon, Yu.F., 1997. Hydrates of Hydrocarbons. PennWell, Tulsa, OK, 488 pp.

Mienert, J., Posewang, J., Baumann, M., 1998. Gas hydrates along the northeastern Atlantic margin: possible hydrate-bound margin instabilities and possible release of methane. In: Henriet, J.-P., Mienert, J. (Eds.), Gas Hydrates: Relevance to World Margin Stability and Climate Change. Geol. Soc. Lond. Spec. Publ. 137, pp. 275–291.

Minshull, T.A., White, R.S., 1989. Sediment compaction and fluid migration in the Makran accretionary prism. J. Geophys. Res. 94, 145–161.

Obzhirov, A., Vereshchagina, O., Winkler, W., 2000. Geochemical methane gas investigations. In: Biebow, N., Lüdmann, T., Karp, B., Kulinich, R. (Eds.), KOMEX: Kurile-Sea of Okhotsk Marine Experiment. Cruise Reports: KOMEX V and KOMEX VI, R/V Professor Gagarinsky Cruise 26 and M/V Marshal Gelovany Cruise 1. GEOMAR Report 88, Kiel, pp. 142–152.

Osborne, M.J., Swarbrick, R.E., 1997. Mechanisms for generating overpressure in sedimentary basins: a reevaluation. Am. Assoc. Pet. Geol. Bull. 81, 1023–1041.

Paull, C.K., Borowski, W.S., Rodriguez, N.M. and the ODP Leg 164 Shipboard Scientific Party, 1998. Marine gas hydrate inventory: preliminary results of ODP leg 164 and implications for gas venting and slumping associated with the Blake Ridge gas hydrate field. In: Henriet, J.-P., Mienert, J. (Eds.), Gas Hydrates: Relevance to World Margin Stability and Climate Change. Geol. Soc. Lond. Spec. Publ. 137, pp. 275–291.

Paull, C.K., Matsumoto, R., Wallace, P.J. and the ODP Leg 164 Shipboard Scientific Party, 1996. Proceedings of the Ocean Drilling Program, Initial Reports Leg 164. Ocean Drilling Program, College Station, TX, 623 pp.

Roberts, H.H., Carney, R.S., 1997. Evidence of episodic fluid, gas and sediment venting on the northern Gulf of Mexico continental slope. Econ. Geol. 92, 863–879.

Ruppel, C., 1997. Anomalously cold temperatures observed at the base of the gas hydrate stability zone on the U.S. Atlantic passive margin. Geology 25, 699–702.

Sancetta, C., 1981. Oceanographic and ecologic significance of diatoms in surface sediments in the Bering Sea and Sea of Okhotsk. Deep-Sea Res. 28, 789–817.

Sandwell, D.T., Smith, W.H.F., 1997. Marine gravity anomaly

from Geosat and ERS1 satellite altimetry. J. Geophys. Res. 102, 10039–10054.

Savostin, L.A., Zonenshain, L., Baranov, B., 1983. Geology and plate tectonics of the Sea of Okhotsk. In: Hilde, T.W.C., Uyeda, S. (Eds.), Geodynamics of the Western Pacific-Indonesian Region. Geodyn. Ser. 11, Washington, DC, pp. 189–222.

Shiga, K., Koizumi, I., 2000. Latest Quaternary oceanographic changes in the Sea of Okhotsk based on diatoms. Mar. Micropaleontol. 38, 91–117.

Soloviev, V., Ginsburg, G.D., 1994. Formation of submarine gas hydrates. Bull. Geol. Soc. Denmark 41, 86–94.

Soloviev, V., Ginsburg, G.D., 1997. Water segregation in the course of gas hydrate formation and accumulation in submarine gas-seepage fields. Mar. Geol. 137, 59–68.

Stoll, R.D., Bryan, G.M., 1979. Physical properties of sediment containing gas hydrates. J. Geophys. Res. 84, 1629–1634.

Talley, L.D., Nagata, Y., 1995. The Sea of Okhotsk and Oyashio Region. 2. North Pacific Marine Science Organization (PICES), PICES Sci. Rep. 2, Sidney, BC, 227 pp.

Taylor, M.H., Dillon, W.P., Pecher, I.A., 2000. Trapping and migration of methane associated with the gas hydrate stability zone at the Blake Ridge Diapir: new insights from seismic data. Mar. Geol. 164, 79–89.

Townend, J., 1997. Estimates of conductive heat flow through bottom-simulating reflectors on the Hikurangi and southwest Fiordland continental margins, New Zealand. Mar. Geol. 141, 209–220.

Van Rensbergen, P., Morley, C.K., Ang, D.W., Hoan, T.Q., Lam, N.T., 1999. Structural evolution of shale diapers from reactive rise to mud volcanism: 3D seismic data from the Baram delta, offshore Brunei Darussalam. J. Geol. Soc. Lond. 156, 633–650.

Wong, H.K., Lüdmann, T., Baranov, B.V., Karp, B. Ya., Konerding, P., Ion, G., 2003. Bottom current-controlled sedimentation and mass wasting in the northwestern Sea of Okhotsk. Mar. Geol. 201, doi:10.1016/S0025-3227(03)-00221-4

Wood, W.T., Gettrust, J.F., 2001. Deep-tow seismic investigation of methane hydrates. In: Paull, C.K., Dillon, W.P. (Eds.), Natural Gas Hydrates: Occurrence, Distribution, and Detection. Geophys. Monogr. 124, pp. 165–178.

Wood, W.T., Ruppel, C., 2000. Seismic and thermal investigations of the Blake Ridge gas hydrate area: a synthesis. In: Paull, C.K., Matsumoto, R., Wallace, P.J., Dillon, W.P. (Eds.), Proceedings of the Ocean Drilling Program, Scientific Results Leg 164. Ocean Drilling Program, College Station, TX, pp. 253–264.

Worrall, D.M., Kruglyak, V., Kunst, F., Kuznetsov, V., 1996. Tertiary tectonics of the Sea of Okhotsk, Russia: Far-field effects of the India-Eurasia collision. Tectonics 4, 813–826.

Yamano, M., Uyeda, S., Aoki, Y.AndShipley,T.H., 1982. Estimates of heat flow derived from gas hydrates. Geology 10, 339–343.

Yun, J.W., Orange, D.L., Field, M.E., 1999. Subsurface gas of northern California and its link to submarine geomorphology. Mar. Geol. 154, 357–368.